PRAMANA
— journal of
physics

Vol. 73, No. 6
December 2009
pp. 1041–1057

Flavour equilibration studies of quark-gluon plasma with non-zero baryon density

ABHIJIT SEN
Department of Physics, Suri Vidyasagar College, Suri 731 101, India
E-mail: abhijisen@yahoo.co.in

MS received 12 March 2008; revised 22 June 2009; accepted 22 June 2009

Abstract. Flavour equilibration for a thermally equilibrated but chemically non-equilibrated quark-gluon plasma is presented. Flavour equilibration is studied enforcing baryon number conservation. In addition to the usual processes like single additional gluon production $gg \rightleftharpoons ggg$ and its reverse and quark–antiquark pair production by gluon pair fusion $gg \rightleftharpoons q_i q_{\bar{i}}$ and reverse thereof, processes like quark-flavour interchanging $q_i q_{\bar{i}} \rightleftharpoons q_j q_{\bar{j}}$ is also considered. The degree of equilibration is studied comparatively for various reactions/constraints that are being considered.

Keywords. Parton; equilibration; baryon number; chemical potential; flavour change.

PACS Nos 12.38.Mh; 21.65; 25.75

1. Introduction

It is known [1] that the initial system produced at RHIC energies have a finite non-zero baryon number density. The antiparticle-to-particle ratio at midrapidity for $\sqrt{s_{NN}} = 130$ GeV Au–Au collisions at the STAR Collaboration, BNL, report a noticeable excess of baryons as compared to antibaryons as reflected by the yields of $\bar{p}/p$ (hovering between 0.6 and 0.8), $\bar{\Lambda}/\Lambda$ (hovering between 0.7 and 0.8) [2] for varying transverse momentum, centrality and rapidity. In a subsequent reporting of the BRAHMS Collaboration, BNL [3], it is seen that during Pb–Pb collisions at $\sqrt{s_{NN}} = 200$ GeV, the $\bar{p}/p$ ratio is a maximum of about 0.8 at zero rapidity and falls off for higher rapidity values.

This excess of baryons (and hence quarks) over antibaryons (and hence antiquarks) clearly necessitates the inclusion of a chemical potential into the theoretical framework. This shall be the main point of emphasis of the present piece of work.

Inclusion of a chemical potential into the framework of parton equilibration studies has been rather recent. Although in 1986, Matsui *et al* [4] reported on strangeness equilibration rates at non-zero chemical potential, it was not until the very end of the past century [5,6] that it was explicitly used in studying chemical equilibration processes. A chemical potential for massless quarks that equalled the system

temperature at all temperatures was assumed by these authors. This however was not very realistic as it did not take into account baryon number conservation. Furthermore, they did not distinguish between quarks and antiquarks.

In 2004, He *et al* [7] undertook a much complete study including baryon number conservation. They used an expansion of the number densities in powers of the chemical potential. They started with a quark–antiquark distinction but that was soon put away.

The present work is in a similar line, but with the following points of difference: (1) we explicitly include the finite strange quark mass, (2) We maintain the quark–antiquark distinction, (3) we use results of full phase space calculations for the pair production and flavour changing processes in contrast with the factorized rates of many earlier works [5–10], (4) for a given initial baryon number density we iterate to obtain the initial value of the quark chemical potential which again evolves obeying the baryon number conservation equation and (5) we study comparatively the degree of equilibration achieved for varying initial conditions.

2. Basic thermodynamics of the system

At this stage, let us note the following points with regard to the chemical potential: (1) Strangeness being conserved in strong interactions and the initial strangeness content of the QGP fireball being zero it implies that strange quark and antiquark are always produced in pairs. This clearly indicates that the strange quark chemical potential is zero. (2) Considering light quark–antiquark pair production processes we can argue that since the net chemical potential on either side of a chemical reaction ought to be the same and gluon chemical potential is zero, this would necessarily imply

$$\mu_q = -\mu_{\bar{q}}.$$

Again, since the mass of u- and d-quarks are nearly equal and much less than that of the strange quark, we can safely treat the lighter flavours in the same footing without any appreciable error being introduced. By a suffix q we shall indicate the lighter quarks in general and treat them as massless.

In order to avoid computational complications we have taken a modified form of the distribution functions instead of the usual full Juttner form. This is in confirmation with earlier works [5,6].

The non-equilibrium distribution functions for the constituent partons of the chemically non-equilibrated state are taken to be

$$f_g = \frac{\lambda_g}{\mathrm{e}^{\varepsilon/T} - 1}, \tag{1a}$$

$$f_{q(\bar{q})} = \frac{\lambda_{q(\bar{q})} \mathrm{e}^{\pm\mu_q/T}}{\mathrm{e}^{\varepsilon/T} + 1} \tag{1b}$$

and

$$f_s = f_{\bar{s}} = \frac{\lambda_s}{\mathrm{e}^{\varepsilon/T} + 1} \tag{1c}$$

where the notations have the usual meanings. Here λ_k gives the ratio of the number density to the equilibrium number density and is termed as the non-equilibrium fugacity for the parton species k. Clearly, for parton equilibration studies, it starts from a low initial value and approaches unity as the system equilibrates.

Of these, the first is the usual Bose distribution function [8], the second is the modified Fermi–Dirac-type distribution function with an exponential term in the numerator to include the light quark chemical potential [5] and the third is the usual modified Fermi–Dirac distribution function for the massive strange quark [8], each being scaled by the non-equilibrium fugacity in order to describe the degree of equilibrium achieved for a chemically equilibrating system.

The rationale for keeping the chemical potential term separate instead of absorbing into the non-equilibrium fugacity as $\lambda_i \to \lambda_i \mathrm{e}^{\mu_i/T}$ are the following:

(1) absorbing the chemical potential would mean that we do not get the time variation of the non-equilibrium fugacity alone, which was one of the main objectives of this study.
(2) We wish to observe the time variation of the fermionic chemical potential, which becomes difficult, if we absorb the chemical potential into the non-equilibrium fugacity.

Using standard rules of statistical mechanics [11] we can obtain the number density n, energy density ε and pressure p of the system. The results are generally represented as

$$t = t_g + n_f(t_q + t_{\bar{q}}) + 2t_s, \tag{2}$$

where $t = n, \varepsilon, p$ with

$$n = \left[\frac{16\zeta(3)}{\pi^2}\lambda_g + \frac{9\zeta(3)n_f}{2\pi^2}(\lambda_q \mathrm{e}^{\mu_q/T} + \lambda_{\bar{q}}\mathrm{e}^{-\mu_q/T}) + \frac{6}{\pi^2}\lambda_s x_s^3 \sum_{k=1}^{\infty}(-1)^{k-1}\frac{K_2(kx_s)}{(kx_s)}\right]T^3 \tag{2a}$$

$$\varepsilon = \left[\frac{8\pi^2}{15}\lambda_g + \frac{7\pi^2 n_f}{40}(\lambda_q \mathrm{e}^{\mu_q/T} + \lambda_{\bar{q}}\mathrm{e}^{-\mu_q/T}) + \frac{6}{\pi^2}\lambda_s x_s^4 \sum_{k=1}^{\infty}(-1)^{k-1}\left\{\frac{3K_2(kx_s)}{(kx_s)^2} + \frac{K_1(kx_s)}{(kx_s)}\right\}\right]T^4 \tag{2b}$$

$$p = \left[\frac{8\pi^2}{45}\lambda_g + \frac{7\pi^2 n_f}{120}(\lambda_q \mathrm{e}^{\mu_q/T} + \lambda_{\bar{q}}\mathrm{e}^{-\mu_q/T}) + \frac{6}{\pi^2}\lambda_s x_s^4 \sum_{k=1}^{\infty}(-1)^{k-1}\frac{K_2(kx_s)}{(kx_s)^2}\right]T^4 \tag{2c}$$

where K_i gives the ith modified Bessel function ($i = 0, 1, 2$), n_f gives the number of massless quark flavours (=2 for our case) and $x_s = m_s/T$.

The baryon number density equals (for two massless quark flavours)

$$n_b = 2\frac{1}{3}(n_q - n_{\bar{q}}). \tag{3}$$

For given initial values of baryon number density, non-equilibrium fugacities and temperature we can iterate to obtain the initial value of the chemical potential. The baryon number conservation equation is given by

$$\partial_\mu(n_b u^\mu) = \frac{\partial n_b}{\partial \tau} + \frac{n_b}{\tau} = 0 \tag{4}$$

which may be expanded to obtain the rate of change of the chemical potential with time. Here, τ is the proper time. We obtain

$$\dot{\mu}_q = \dot{\lambda}_q B_1 + \dot{\lambda}_{\bar{q}} B_2 + \dot{T} B_3 + B_4, \tag{5}$$

where

$$B_1 = \frac{-T\mathrm{e}^{\mu_q/T}}{\lambda_q \mathrm{e}^{\mu_q/T} + \lambda_{\bar{q}}\mathrm{e}^{-\mu_q/T}} \tag{5a}$$

$$B_2 = \frac{T\mathrm{e}^{-\mu_q/T}}{\lambda_q \mathrm{e}^{\mu_q/T} + \lambda_{\bar{q}}\mathrm{e}^{-\mu_q/T}} \tag{5b}$$

$$B_3 = \frac{\mu_q}{T} - 3\frac{\lambda_q \mathrm{e}^{\mu_q/T} - \lambda_{\bar{q}}\mathrm{e}^{-\mu_q/T}}{\lambda_q \mathrm{e}^{\mu_q/T} + \lambda_{\bar{q}}\mathrm{e}^{-\mu_q/T}} \tag{5c}$$

and

$$B_4 = -\frac{T(\lambda_q \mathrm{e}^{\mu_q/T} - \lambda_{\bar{q}}\mathrm{e}^{-\mu_q/T})}{\tau(\lambda_q \mathrm{e}^{\mu_q/T} + \lambda_{\bar{q}}\mathrm{e}^{-\mu_q/T})}. \tag{5d}$$

It is to be noted here that for a baryon-free plasma $\dot{\mu}_q$ vanishes. As we shall see shortly, due to these non-zero coefficients, the light quark and antiquark number density evolution equations get coupled with one another.

3. Parton equilibration equations

Assuming longitudinal boost invariance, the fundamental equation that dictates the parton number density evolution is given by

$$\partial_\mu(n_k u^\mu) = \frac{\partial n_k}{\partial \tau} + \frac{n_k}{\tau} = (R_{\mathrm{gain}} - R_{\mathrm{loss}}), \tag{6}$$

where the RHS gives the difference of rate of gain and loss of the parton species k for the reaction mentioned, i.e. the net rate of change of the number density. Here, as before, τ is the proper time. Using standard procedures [10,11], substituting for

the different partonic number densities and the various reactions considered, this equation leads to the parton number density evolution equations as we shall see shortly.

The gluon number density evolution equation is given as

$$\partial_\mu(n_g u^\mu) = (R_{gg\to ggg} - R_{ggg\to gg}) - \sum_i (R_{gg\to i\bar{i}} - R_{i\bar{i}\to gg}), \tag{7}$$

where the sum is over all quark flavours present. Substituting for the gluon number density and substituting for the rates we have

$$\dot{\lambda}_g G_1 + \dot{T} G_2 + G_3 = 0, \tag{8}$$

where $G_1 = 1/\lambda_g$, $G_2 = 3/T$ and $G_3 = (1/\tau) - (R_3(1-\lambda_g) - \sum_i R_{2i}/n_g)$, where as in earlier works [8,10,11] we have introduced rates R_{2i} and R_3 for the rates in (7) above. We shall look more closely at these rates soon.

As mentioned earlier, due to the coefficients B_i, the light quark and antiquark number density evolution equations get coupled to each other. We obtain the following results:

For the light quarks the equation is given by

$$\dot{\lambda}_q Q_1 + \dot{\lambda}_{\bar{q}} Q_2 + \dot{T} Q_3 + Q_4 = 0, \tag{9}$$

where

$$Q_1 = \frac{1}{\lambda_q} + \frac{B_1}{T}, \tag{9a}$$

$$Q_2 = \frac{B_2}{T}, \tag{9b}$$

$$Q_3 = \frac{3}{T} + \frac{B_3}{T} - \frac{\mu_q}{T^2}, \tag{9c}$$

$$Q_4 = \frac{1}{\tau} + \frac{B_4}{T} - SQ \tag{9d}$$

with

$$SQ = \{(R_{gg\to q\bar{q}} - R_{q\bar{q}\to gg})/n_q\} - \{(R_{q\bar{q}\to s\bar{s}} - R_{s\bar{s}\to q\bar{q}})/n_q\} \tag{9e}$$

for light quarks.

For the antiquark case, we obtain the equation as

$$\dot{\lambda}_q AQ_1 + \dot{\lambda}_{\bar{q}} AQ_2 + \dot{T} AQ_3 + AQ_4 = 0 \tag{10}$$

where

$$AQ_1 = -\frac{B_1}{T} \tag{10a}$$

$$AQ_2 = \frac{1}{\lambda_{\bar{q}}} - \frac{B_2}{T} \tag{10b}$$

$$AQ_3 = \frac{3}{T} - \frac{B_3}{T} + \frac{\mu_q}{T^2} \tag{10c}$$

$$AQ_4 = \frac{1}{\tau} - \frac{B_4}{T} - SaQ \tag{10d}$$

with

$$SaQ = \{(R_{gg\to q\bar{q}} - R_{q\bar{q}\to gg})/n_{\bar{q}}\} - \{(R_{q\bar{q}\to s\bar{s}} - R_{s\bar{s}\to q\bar{q}})/n_{\bar{q}}\} \tag{10e}$$

for light antiquarks.

For massive strange quark the equation takes the form

$$\dot{\lambda}_s S_1 + \dot{T} S_2 + S_3 = 0, \tag{11}$$

where

$$S_1 = \frac{1}{\lambda_s} \tag{11a}$$

$$S_2 = \frac{3}{T} \frac{\sum_{k=1}^{\infty} (-1)^{k-1} \left\{ \frac{3K_2(kx_s)}{(kx_s)^2} + \frac{K_1(kx_s)}{(kx_s)} \right\}}{\sum_{k=1}^{\infty} (-1)^{k-1} \frac{K_2(kx_s)}{(kx_s)}} \tag{11b}$$

$$S_3 = \frac{1}{\tau} - SQs \tag{11c}$$

with

$$SQs = \{(R_{gg\to s\bar{s}} - R_{s\bar{s}\to gg})/n_s\} + 2\{(R_{q\bar{q}\to s\bar{s}} - R_{s\bar{s}\to q\bar{q}})/n_s\} \tag{11d}$$

for strange quarks.

From the energy–momentum conservation equation

$$\partial_\mu T^{\mu\nu} = 0 \tag{12}$$

we obtain for $(1+1)D$

$$\frac{\mathrm{d}\varepsilon}{\mathrm{d}\tau} + \frac{\varepsilon + p}{\tau} = 0 \tag{13}$$

(which we shall refer to as Bjorken's equation henceforth). We get on substituting for energy and momentum

$$\dot{T} f_6 + \dot{\lambda}_g f_7 + \dot{\lambda}_q f_8 + \dot{\lambda}_{\bar{q}} f_9 + \dot{\lambda}_s f_s + f_{10} = 0, \tag{14}$$

where the f_i's are functions of the non-equilibrium fugacities, temperature and light quark chemical potential. The full expressions of the f_i's can be found in Appendix A.

To obtain the time variation of the non-equilibrium fugacities, we require to solve coupled differential equations (8)–(11) and (14) simultaneously. We have done the same using Runge–Kutta techniques. However, there remains a very important point to mention regarding the evaluation of the rate of change of the chemical potential. Since the baryon number conservation equation is obtained directly from the quark and antiquark number densities, as are the massless quark and antiquark number density evolution equations, these two evolution equations (coupled by the four B-coefficients) along with the energy–momentum conservation equation (with substitutions for $\dot{\lambda}_s$, $\dot{\lambda}_g$ from the respective number density evolution equations) do not generate a set of solvable coupled equations for $\dot{\lambda}_q$, $\dot{\lambda}_{\bar{q}}$, $\dot{T}$ as the system determinant vanishes.

To tackle this problem of unsolvability, we adopt an approximation scheme. While evaluating B_j $(j = 1, 2)$ we use a truncated form of the expansion of the exponential in the numerator keeping the rest of the B-terms unchanged. Although this prescription is expected to work, strictly speaking, this however would not mean exact baryon number conservation. The more number of terms we take of the expansion, the more realistic it is expected to be.

4. Parton equilibration rates

The gluon multiplication rate has been calculated by Xiong and Shuryak [12]. By explicitly calculating the matrix element [13] (summed over the final states and averaged over initial states) we can obtain the gluon multiplication rate. However, to avoid the huge calculations of evaluating 25 Feynman diagrams [13] involved, we fall back on the treatments used in earlier works [6,11]. We postulate that the gluon multiplication rate depends on the chemical potential via the Debye screening mass.

The Debye screening mass suitable for a multicomponent chemically non-equilibrated parton plasma is given by [14]

$$m_{\mathrm{D}}^2 = \frac{2g^2}{\pi^2} \int \mathrm{d}k\, k \left[N_{\mathrm{c}} f_g + \sum_i f_i \right], \tag{15}$$

where the sum runs over all flavours i, while N_{c} gives the number of colours. To accommodate for antiquarks and remembering that our number of flavours is 3 and not 6, we propose the following modification:

$$m_{\mathrm{D}}^2 = \frac{2g^2}{\pi^2} \int \mathrm{d}k\, k \left[3 f_g + \frac{1}{2} \sum_{i=u,d,s} (f_i + f_{\bar{i}}) \right]. \tag{15a}$$

Here

$$g^2 = 4\pi\alpha_s, \tag{15b}$$

where α_s is the temperature-dependent strong coupling constant, given by

$$\alpha_s = \frac{12\pi}{(33 - 2X3)\ln(Q^2/\Lambda_0^2)} \tag{15c}$$

with the parameters $Q = 2\pi T$ and $\Lambda_0 = 300$ MeV. Alternatively, as an approximation, a temperature-independent value of 0.3 could also be used for the strong coupling constant α_s.

Using standard techniques [5,6,8,11] we can obtain the following result for the mean free path λ_f:

$$\lambda_f^{-1} = n_g \int \mathrm{d}q_\perp^2 \frac{\mathrm{d}\sigma_{el}^{gg}}{\mathrm{d}q_\perp^2} = n_g \int_0^{s/4} \mathrm{d}q_\perp^2 \frac{9}{4} \frac{2\pi\alpha_s^2}{(q_\perp^2 + m_\mathrm{D}^2)^2} = \frac{9 n_g \pi \alpha_s^2}{2m_\mathrm{D}^2 (1 + \frac{2}{9}\frac{m_\mathrm{D}^2}{T^2})} \tag{16}$$

which for zero chemical potential case reduces to the well-known [8,11] result:

$$\lambda_f^{-1} = \frac{9}{8} a_1 \alpha_s T \frac{1}{1 + 8\pi\alpha_s \lambda_g/9} \tag{16a}$$

using

$$m_\mathrm{D}^2 = 4\pi\alpha_s T^2 \lambda_g. \tag{16b}$$

In eq. (16) we have used the result for the regularized small angle gg scattering cross-section

$$\frac{\mathrm{d}\sigma_{el}^{gg}}{\mathrm{d}q_\perp^2} = \frac{9}{4} \frac{2\pi\alpha_s^2}{(q_\perp^2 + m_\mathrm{D}^2)^2}. \tag{17}$$

The regularized gluon density distribution induced by a single scattering is given by

$$\frac{\mathrm{d}n_g}{\mathrm{d}^2 k_\perp \mathrm{d}y} = \frac{3\alpha_s}{\pi^2} \frac{q_\perp^2}{k_\perp^2 [(\vec{k}_\perp - \vec{q}_\perp)^2 + m_\mathrm{D}^2]}. \tag{18}$$

Using standard methods [5,6,8,11] we get the modified differential cross-section as

$$\frac{\mathrm{d}\sigma_3}{\mathrm{d}q_\perp^2 \mathrm{d}^2 k_\perp \mathrm{d}y} = \frac{\mathrm{d}\sigma_{el}^{gg}}{\mathrm{d}q_\perp^2} \frac{\mathrm{d}n_g}{\mathrm{d}^2 k_\perp \mathrm{d}y} \theta\left(\lambda_f - \frac{\cosh y}{k_\perp}\right) \theta(\sqrt{s} - k_\perp \cosh y). \tag{19}$$

Here, the first step function includes the approximate LPM suppression of the induced gluon and the second step function accounts for energy conservation. Here $k_\perp$ denotes the transverse momentum, y denotes the rapidity of the radiated gluon and $q_\perp$ denotes the momentum transfer in the elastic collisions.

The infrared divergence associated with the QCD radiation is regularized by the LPM effect. There still remain in (19) infrared singularities in both the scattering cross-sections and radiation amplitudes associated with the gluon propagator.

These are approximately controlled by introducing the Debye screening mass, as obtained earlier.

Recalling the definition of

$$R_3 = \frac{1}{2}\sigma_3 n_g \tag{20}$$

with

$$\sigma_3 = \langle \sigma(gg \to ggg)v \rangle \tag{21}$$

the thermally averaged velocity weighted cross-section, we obtain the required rate as

$$\frac{R_3}{T} = \frac{27\alpha_s^3}{2}\lambda_f^2 n_g I(\lambda_g), \tag{22}$$

where

$$I(\lambda_g) = \int_1^{\sqrt{s}\lambda_f} \mathrm{d}x \int_0^{\frac{s}{4m_\mathrm{D}^2}} \mathrm{d}z \frac{z}{(1+z)^2} \left[\frac{\cosh^{-1}\sqrt{x}}{x\sqrt{[x+(1+z)x_\mathrm{D}]^2 - 4xzx_\mathrm{D}}} + \frac{1}{s\lambda_f^2} \frac{\cosh^{-1}\sqrt{x}}{\sqrt{[1+x(1+z)y_\mathrm{D}]^2 - 4xzy_\mathrm{D}}} \right] \tag{23}$$

with

$$x_\mathrm{D} = m_\mathrm{D}^2 \lambda_f, \quad y_\mathrm{D} = \frac{m_\mathrm{D}^2}{s}. \tag{24}$$

We have parton production rates in the RHS of the number density evolution equations. Let us evaluate the quark–antiquark pair production reaction rate R_{2q}. We have [4]

$$R_{2q} = R_{\mathrm{gain}}^{gg} - R_{\mathrm{loss}}^{gg}, \tag{25}$$

where

$$R_{\mathrm{gain}}^{gg} = \int \frac{\mathrm{d}^3p_1}{(2\pi)^3 2E_1} \int \frac{\mathrm{d}^3p_2}{(2\pi)^3 2E_2} \int \frac{\mathrm{d}^3p_3}{(2\pi)^3 2E_3} \int \frac{\mathrm{d}^3p_4}{(2\pi)^3 2E_4} (2\pi)^4 \times \delta^4(p_1+p_2-p_3-p_4)\Sigma|M_{gg\to i\bar{i}}|^2 f_g(p_1) f_g(p_2) \times (1-f_q(p_3))(1-f_{\bar{q}}(p_4)) \tag{25a}$$

and

$$R_{\mathrm{loss}}^{gg} = \int \frac{\mathrm{d}^3p_1}{(2\pi)^3 2E_1} \int \frac{\mathrm{d}^3p_2}{(2\pi)^3 2E_2} \int \frac{\mathrm{d}^3p_3}{(2\pi)^3 2E_3} \int \frac{\mathrm{d}^3p_4}{(2\pi)^3 2E_4} (2\pi)^4 \times \delta^4(p_1+p_2-p_3-p_4)\Sigma|M_{gg\to i\bar{i}}|^2 (1+f_g(p_1)) \times (1+f_g(p_2)) f_q(p_3) f_{\bar{q}}(p_4). \tag{25b}$$

The recasting of eq. (25) with inputs from eqs (25a) and (25b) are given in Appendix B.

Identically, for the quark flavour changing process we have [4]

$$R_{qg} = R^{q\bar{q}}_{\text{gain}} - R^{q\bar{q}}_{\text{loss}}, \tag{26}$$

where

$$\begin{aligned} R^{q\bar{q}}_{\text{gain}} = & \int \frac{\mathrm{d}^3 p_1}{(2\pi)^3 2E_1} \int \frac{\mathrm{d}^3 p_2}{(2\pi)^3 2E_2} \int \frac{\mathrm{d}^3 p_3}{(2\pi)^3 2E_3} \int \frac{\mathrm{d}^3 p_4}{(2\pi)^3 2E_4} (2\pi)^4 \\ & \times \delta^4(p_1 + p_2 - p_3 - p_4) \Sigma |M_{s\bar{s}\to q\bar{q}}|^2 \\ & \times f_q(p_1) f_{\bar{q}}(p_2)(1 - f_s(p_3))(1 - f_{\bar{s}}(p_4)) \end{aligned} \tag{26a}$$

and

$$\begin{aligned} R^{q\bar{q}}_{\text{loss}} = & \int \frac{\mathrm{d}^3 p_1}{(2\pi)^3 2E_1} \int \frac{\mathrm{d}^3 p_2}{(2\pi)^3 2E_2} \int \frac{\mathrm{d}^3 p_3}{(2\pi)^3 2E_3} \int \frac{\mathrm{d}^3 p_4}{(2\pi)^3 2E_4} (2\pi)^4 \\ & \times \delta^4(p_1 + p_2 - p_3 - p_4) \Sigma |M_{s\bar{s}\to q\bar{q}}|^2 \\ & \times (1 - f_q(p_1))(1 - f_{\bar{q}}(p_2)) f_s(p_3) f_{\bar{s}}(p_4). \end{aligned} \tag{26b}$$

The recasting of eq. (26) with inputs from eqs (26a) and (26b) are given in Appendix C.

5. Results

5.1 *Initial conditions*

As an initial condition at the point of thermalization (i.e. the point after which the system evolves according to the laws of hydrodynamics) we have predictions from the HIJING and SSPC models [15]. In addition to these inputs we shall require inputs for at least two of the following: initial baryon number density, initial light quark chemical potential and ratio of the initial non-equilibrium fugacities of light quarks and antiquarks.

In the absence of initial values thereof (although we have some initial conditions calculated at $\tau_i = 0.1$ fm/c [1,16], which is at a much earlier time than the time of thermalization at $\tau_i = 0.25$ fm/c for SSPC initial conditions and earlier still for HIJING at $\tau_i = 0.6 - 0.7$ fm/c [15]) let us study the relative degree of equilibration for varying initial conditions although it must be emphasized that most of these initial conditions would be of purely academic interest only, as they cannot be realized in practice at the collider experiments. Nevertheless, it is hoped that this exercise would pave the way for a clearer understanding of the physical processes involved.

Even though two inputs remain rather arbitrary, we use both sets of initial conditions (LHC and RHIC) to study the trends. For the usual inputs we use the following sets of data (SSPC):

LHC

τ_i (fm/c)	T (GeV)	λ_g	λ_q	λ_s
0.25	1.02	0.43	0.086	0.043

RHIC

τ_i (fm/c)	T (GeV)	λ_g	λ_q	λ_s
0.25	0.668	0.34	0.064	0.032

As a representative plot we use baryon density $0.15/\text{fm}^3$ and ratio $= 1.5$ with the initial conditions as given above. We also try to see the effect of including the quark flavour changing processes (QFCP). We continue the evolution till the temperature falls below 0.17 GeV.

5.2 *Observed trends*

We study comparatively the outputs with given initial baryon number density and initial light quark-to-antiquark fugacity ratio. We vary the baryon number density between $0.21/\text{fm}^3$ and $0.11/\text{fm}^4$ while we change the ratio between 1.9 and 1.1. We arrive at the following conclusions:

(1) The nature of variations of the physical quantities are more or less in the line of earlier works. The results for RHIC and LHC initial conditions are shown in figures 1 and 2 respectively. Temperature, chemical potential and non-equilibrium fugacity variations with RHIC initial conditions are given in figure 1 while that for LHC are given in figure 2. As reported in all previous works [5–10,18] the QGP remains far away from full chemical equilibration.

(2) The decaying curves give temperature variations while the positive rising curves are sequentially (from top) for gluon, light quark, light antiquark and strange quark fugacity variations. Plots for both 'quark flavour changing process' included and excluded cases are shown. For identification, please see point 5 below.

We observe that (i) as expected, the temperature falls with time while the non-equilibrium fugacities increase, (ii) contrary to the Juttner case, the chemical potential remains negative all along and as expected approaches zero as the system equilibrates. Some results for the full Juttner distribution functions can be found in [17], (iii) the QGP, as expected remains to be gluon-dominated and (iv) for a system at higher chemical potential, the temperature falls at a slower rate signifying lesser amount of energy expenditure to create partons which shows up in the slower rise of all partons except for the light antiquark, which shows a larger growth rate due to the presence of the exponentiated chemical potential.

(3) For a given initial ratio, except for the light quarks and antiquarks, the output does not depend much on the initial baryon number density. For the light quarks and antiquarks this variation is due to the presence of the respective non-zero chemical potentials.

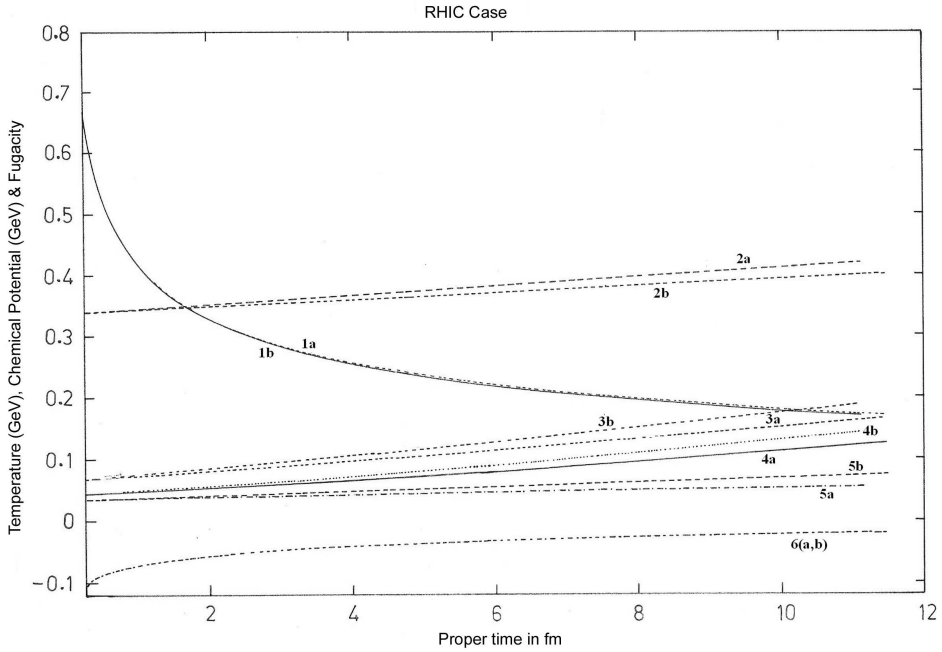

Figure 1. The temperature, chemical potential and non-equilibrium fugacity variations for RHIC initial conditions. Curve 1a: Temperature variation for QFCP excluded case, curve 1b: temperature variation for QFCP included case, curve 2a: gluon fugacity variation for QFCP included case, curve 2b: gluon fugacity variation for QFCP excluded case, curve 3a: light quark fugacity variation for QFCP included case, curve 3b: light quark fugacity variation for QFCP excluded case, curve 4a: light antiquark fugacity variation for QFCP included case, curve 4b: light antiquark fugacity variation for QFCP excluded case, curve 5a: strange quark fugacity variation for QFCP excluded case, curve 5b: strange quark fugacity variation for QFCP included case and curve 6(a,b): light quark chemical potential variation for QFCP excluded and included cases (practically coincident).

(4) For a given initial baryon number density we can recast (3), the equation for baryon number density, with inputs from (2a) for the number densities, in the form

$$\mathrm{e}^{\mu_q/T} = \frac{C}{2\lambda_q} + \sqrt{\frac{1}{D} + \frac{C^2}{4\lambda_q^2}}, \tag{27}$$

where C is a constant for a given temperature, light quark fugacity and given baryon number density. Here D is the light quark-to-antiquark initial fugacity ratio. For a fixed light quark fugacity and temperature, as D falls clearly the RHS of the above equation increases which indicates a rise in the chemical potential. Again for a system of higher chemical potential, the temperature has to drop at a slower rate due to the constraint imposed. Hence we observe that (i) the temperature falls at a slower rate for a smaller value of the light quark-to-antiquark initial fugacity ratio,

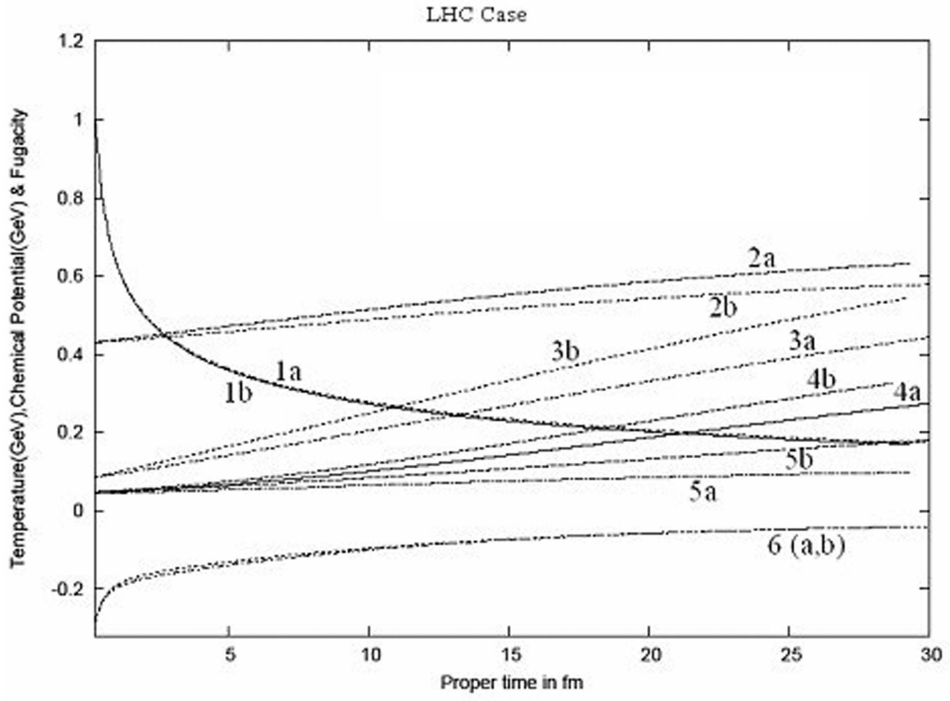

Figure 2. Same as for figure 1 but for LHC initial conditions.

(ii) as the temperature falls at a slower rate, it would imply a lesser expenditure of energy to produce particles in general. This would show up in the slower rise of all fugacity values except the light antiquark, which would show a higher growth rate. This is due to the exponentiated chemical potential part.

(5) For inclusion of the quark-flavour-changing process we observe the following: Due to the additional production of s-quarks from massless quarks via QFCP, we see an additional increase in fugacity of the strange quark while, the rate of equilibration falls for all other non-strange quarks. Due to the additional expenditure of energy to create more massive s-quarks, the temperature falls at a faster rate.

(6) For the chemical potential of the light quarks, clearly the value thereof starts from a low value as obtained by iteration to fit the initial condition and evolves according to the baryon number conservation equation. It tends to level off as the system equilibrates. The chemical potential remains negative all along, which can be attributed to the choice of the distribution function.

Appendix A: Bjorken's equation

Bjorken's equation $\frac{\mathrm{d}\varepsilon}{\mathrm{d}\tau} + \frac{\varepsilon+p}{\tau} = 0$ when expanded took the form

$$\dot{T} f_6 + \dot{\lambda}_g f_7 + \dot{\lambda}_q f_8 + \dot{\lambda}_{\bar{q}} f_9 + \dot{\lambda}_s f_s + f_{10} = 0. \tag{A1}$$

Here

$$f_6 = \frac{32\pi^2}{15}\lambda_g T^3 + \frac{7\pi^2}{20}(\lambda_q \mathrm{e}^{\mu_q/T} - \lambda_{\bar{q}}\mathrm{e}^{-\mu_q/T})\left(\frac{B_3}{T} - \frac{\mu_q}{T^2}\right)T^4 + \frac{28\pi^2}{20}(\lambda_q \mathrm{e}^{\mu_q/T} + \lambda_{\bar{q}}\mathrm{e}^{-\mu_q/T})T^3 + \frac{72}{\pi^2 T}m_s^4\lambda_s \times \left\{\frac{K_2(kx_s)}{(kx_s)^2} + \frac{5K_1(kx_s)}{12(kx_s)} + \frac{K_0(kx_s)}{12}\right\}, \tag{A1a}$$

$$f_7 = \frac{8\pi^2}{15}T^4, \tag{A1b}$$

$$f_s = \frac{6}{\pi^2}m_s^4\sum_{k=1}^{\infty}(-1)^{k-1}\left\{\frac{3K_2(kx_s)}{(kx_s)^2} + \frac{K_1(kx_s)}{(kx_s)}\right\}, \tag{A1c}$$

$$f_8 = \frac{7\pi^2}{20}\mathrm{e}^{\mu_q/T}T^4 + \frac{7\pi^2}{20}(\lambda_q \mathrm{e}^{\mu_q/T} - \lambda_{\bar{q}}\mathrm{e}^{-\mu_q/T})\frac{B_1}{T}T^4, \tag{A1d}$$

$$f_9 = \frac{7\pi^2}{20}\mathrm{e}^{-\mu_q/T}T^4 + \frac{7\pi^2}{20}(\lambda_q \mathrm{e}^{\mu_q/T} - \lambda_{\bar{q}}\mathrm{e}^{-\mu_q/T})\frac{B_2}{T}T^4, \tag{A1e}$$

$$f_{10} = \frac{32\pi^2}{45\tau}\lambda_g T^4 + \frac{28\pi^2}{60\tau}(\lambda_q \mathrm{e}^{\mu_q/T} + \lambda_{\bar{q}}\mathrm{e}^{-\mu_q/T})T^4 + \frac{6m_s^4}{\pi^2\tau}\lambda_s\sum_{k=1}^{\infty}(-1)^{k-1}\left\{\frac{4K_2(kx_s)}{(kx_s)^2} + \frac{K_1(kx_s)}{(kx_s)}\right\} + \frac{7\pi^2}{20}(\lambda_q \mathrm{e}^{\mu_q/T} - \lambda_{\bar{q}}\mathrm{e}^{-\mu_q/T})\frac{B_4}{T}T^4, \tag{A1f}$$

where all symbols have usual meanings.

Appendix B: Gluon pair fusion reaction rate

Following [4], we can say that there are three topologically distinct Feynmann diagrams that contribute towards the quark–antiquark pair production process. Evaluating them, performing traces and finally adding them up we can find the net squared matrix element. We basically follow the lines of [4]. Transforming variables as

$$q = p_1 + p_2, \quad p = \frac{1}{2}(p_1 - p_2)$$
$$q' = p_3 + p_4, \quad p' = \frac{1}{2}(p_3 - p_4) \tag{B1}$$

with restrictions

$$
\begin{aligned}
&q_0 > 2m_i \\
&s = q_0^2 - |\vec{\mathbf{q}}|^2 \geq 4m_i^2 \\
&p_0^2 \leq \frac{q^2}{4} \\
&p_0' p_0' \leq \frac{q^2}{4}\left(1 - \frac{4m_i^2}{s}\right)
\end{aligned} \tag{B2}
$$

and transforming the three-dimensional integrals to four-dimensional integrals using

$$
\int \frac{\mathrm{d}^3 p_i}{2E_i} = \int \mathrm{d}^4 p_i \delta(p^2 - m_i^2) \tag{B3}
$$

with the new set of variables

$$
\begin{aligned}
&q_0 = -T \ln v + 2m_i \\
&q^{1/2} = (q_0^2 - 4m_i^2)^{1/2} u \\
&p_0 = \frac{q}{2}\left(1 - \frac{4m_i^2}{s}\right)^{1/2} x \\
&p_0' = \frac{q}{2} y
\end{aligned} \tag{B4}
$$

we arrive at the rate

$$
\begin{aligned}
R_{2g} = \frac{\alpha_s^2}{2\pi^3} T \int_0^1 \mathrm{d}u \int_0^1 \mathrm{d}v \int_0^1 \mathrm{d}x \int_0^1 \mathrm{d}y \frac{u^2}{v} \\
\times \left(1 - \frac{4m_i^2}{s}\right)^{1/2} (q_0^2 - 4m_i^2)^{3/2} f_{\text{Quarks}} f_{\text{phase 1}}
\end{aligned} \tag{B5}
$$

where

$$
\begin{aligned}
f_{\text{Quarks}} = {} & f_g\left(\frac{q_0}{2} + p_0\right) f_g\left(\frac{q_0}{2} - p_0\right)\left(1 - f_q\left(\frac{q_0}{2} + p_0'\right)\right) \\
& \times \left(1 - f_{\bar{q}}\left(\frac{q_0}{2} - p_0'\right)\right) - \left(1 + f_g\left(\frac{q_0}{2} + p_0\right)\right) \\
& \times \left(1 + f_g\left(\frac{q_0}{2} - p_0\right)\right) f_q\left(\frac{q_0}{2} + p_0'\right) f_{\bar{q}}\left(\frac{q_0}{2} - p_0'\right)
\end{aligned} \tag{B5a}
$$

and

$$
f_{\text{phase 1}} = A + B\left[\frac{1}{K_+} + \frac{1}{K_-}\right] + C\left[\frac{\Delta_+}{K_+^3} + \frac{\Delta_-}{K_+^3}\right] \tag{B5b}
$$

with

$$
A = 3\left[1 - \left[1 - \frac{4m_i^2}{s}\right]\left[\frac{(1-x^2)(1-y^2)}{2} + x^2 y^2\right]\right] - \frac{34}{3} - 24\frac{m_i^2}{s} \tag{B5c}
$$

$$B = \frac{16}{3}\left[1 + \frac{4m_i^2}{s} + \frac{m_i^4}{s^2}\right] \tag{B5d}$$

$$C = -\frac{128}{3}\frac{m_i^4}{s^2} \tag{B5e}$$

$$K_\pm = \left[1 - \left[1 - \frac{4m_i^2}{s}\right](1 - x^2 - y^2) \pm 2\left[1 - \frac{4m_i^2}{s}\right]^{1/2} xy\right]^{1/2} \tag{B5f}$$

$$\Delta_\pm = 1 \pm \left[1 - \frac{4m_i^2}{s}\right]^{1/2} xy. \tag{B5g}$$

Appendix C: Quark flavour changing process

Following [4], we can say that there is only one type of topologically distinct Feynmann diagram that contributes towards the quark-flavour-changing process or the strange quark pair production process. Evaluating it, and performing trace calculations we can find the squared matrix element. We basically follow the lines of [4]. Transforming variables as in the case before and performing identical operations we can get the rate as

$$\begin{aligned} R_{qg} = {} & \frac{\alpha_s^2}{2\pi^3} T \int_0^1 \mathrm{d}u \int_0^1 \mathrm{d}v \int_0^1 \mathrm{d}x \int_0^1 \mathrm{d}y \frac{u^2}{v} \\ & \times \left(1 - \frac{4m_i^2}{s}\right)^{1/2} (q_0^2 - 4m_i^2)^{3/2} f_{\text{Strange}} f_{\text{phase 2}} \end{aligned} \tag{C1}$$

with

$$\begin{aligned} f_{\text{Quarks}} = {} & f_q\left(\frac{q_0}{2} + p_0\right) f_{\bar{q}}\left(\frac{q_0}{2} - p_0\right)\left(1 - f_s\left(\frac{q_0}{2} + p_0'\right)\right) \\ & \times \left(1 - f_{\bar{s}}\left(\frac{q_0}{2} - p_0'\right)\right) - \left(1 - f_q\left(\frac{q_0}{2} + p_0\right)\right) \\ & \times \left(1 - f_{\bar{q}}\left(\frac{q_0}{2} - p_0\right)\right) f_s\left(\frac{q_0}{2} + p_0'\right) f_{\bar{s}}\left(\frac{q_0}{2} - p_0'\right), \end{aligned} \tag{C1a}$$

$$f_{\text{phase 2}} = \left[1 + \left[1 - \frac{4m_i^2}{s}\right]\left[\frac{(1-x^2)(1-y^2)}{2} + x^2y^2\right]\right] + \frac{4m_i^2}{s}. \tag{C1b}$$

Acknowledgement

The author gratefully acknowledges helpful discussions with Prof. Bikash Sinha and Prof. Binayak Dutta Roy as also valuable e-mail clarifications and encouragement from Professors Z J He and Y G Ma during the initial stages of the present work.

The author also gratefully acknowledges guidelines from the anonymous referee(s) regarding the layout of the present paper.

References

[1] N Hammon, H Stocker and W Greiner, *Phys. Rev.* **C61**, 014901 (1999)
[2] STAR Collaboration, *Phys. Lett.* **B567**, 167 (2003)
[3] BRAHMS Collaboration, *Phys. Lett.* **B607**, 42 (2005)
[4] T Matsui, B Svetitsky and L D McLerran, *Phys. Rev.* **D34**, 783 (1986)
[5] D Dutta, A K Mohanty, K Kumar and R K Choudhury, *Phys. Rev.* **C60**, 014905 (1999)
[6] D Dutta, A K Mohanty, K Kumar and R K Choudhury, *Phys. Rev.* **C61**, 064911 (2000)
[7] Z J He, J L Long, Y G Ma, G L Ma and B Liu, *Phys. Rev.* **C69**, 034906 (2004)
[8] Dipali Pal, Abhijit Sen, Munshi Golam Mustafa and Dinesh Kumar Srivastava, *Phys. Rev.* **C65**, 034901 (2002)
[9] T S Biro, E van Doorn, B Muller, M H Thoma and X N Wang, *Phys. Rev.* **C48**, 1275 (1993)
[10] Peter Levai and X-N Wang, *Proceedings of Strangeness '95*, Tucson, Arizona, USA, Jan. 4–6, 1995, Am. Inst. of Phys.
[11] *Introduction to high energy heavy ion collisions* edited by C Y Wong (World Scientific, 1994), Ch. 9
[12] Li Xiong and Edward V Shuryak, *Phys. Rev.* **C49**, 2203 (1994)
[13] F A Berends, R Kliess, P De Causmaecker, R Gastmans and Tai Tsun Wu, *Phys. Lett.* **B103**, 124 (1981)
[14] Fred Cooper, Chung Wen Kao and Gouranga C Nayak, arXiv.org/hep-ph/0207370 and references therein
[15] Munshi G Mustafa and Markus H Thoma, *Phys. Rev.* **C62**, 014902 (2000)
[16] E J Eskola, *Prog. Theo. Phys. Suppl.* **129**, 1 (1997)
[17] Abhijit Sen, arXiv.org/0802.3743
[18] J Alam, P Roy, S Sarkar, S Raha and B Sinha, *Int. J. Mod. Phys.* **A12(28)**, 5151 (1997)